

# The anti-ordinary Hall effect in NiPt thin films

Taras Golod,<sup>1</sup> Andreas Rydh,<sup>1</sup> Peter Svedlindh,<sup>2</sup> and Vladimir M. Krasnov<sup>1,\*</sup>

<sup>1</sup>*Department of Physics, Stockholm University, AlbaNova University Center, SE-10691 Stockholm, Sweden*

<sup>2</sup>*Department of Engineering Sciences, Uppsala University, Box 534, SE-75121 Uppsala, Sweden*

(Dated: June 18, 2018)

We study the anomalous Hall effect in binary alloys between the group-10 elements Ni and Pt. It is observed that the ordinary Hall effect is negative (electron-like) at any composition of the alloy. The extraordinary Hall effect is also negative except in the vicinity of the ferromagnetic quantum critical point. Close to the critical point the sign of the extraordinary Hall effect can be changed to positive (hole-like) by tuning either the temperature or the composition of the alloy. We attribute such an “anti-ordinary” Hall effect with opposite signs of the ordinary and the extraordinary contributions to a Berry phase singularity, moving away from the Fermi energy with increasing the ferromagnetic exchange energy.

Hall effect in ferromagnetic metals comprises the ordinary and the extraordinary contributions, proportional to the applied magnetic field  $H$  and the magnetization  $M$ , respectively [1]:

$$\rho_{xy} = R_0 H + R_1 M. \quad (1)$$

Here  $R_0$  and  $R_1$  are the ordinary and the extraordinary Hall coefficients. The ordinary Hall effect (OHE) is caused by the action of the spin-independent Lorentz force on itinerant charge carriers. The sign of the OHE reflects the topology of the Fermi surface [2], it is negative for electron-like and positive for hole-like charge carriers. The extraordinary Hall effect (EHE) arises from various spin-orbit interactions [1]. However, the mechanisms of the extraordinary Hall effect (EHE) are still under debate [3–7], making the EHE possibly the oldest unsolved problem in solid state physics. Identification of the EHE mechanisms is obscured by the coexistence of intrinsic (electron-structure related) [8] and extrinsic (impurity and scattering related) [9–12] contributions that are difficult to disentangle.

NiPt alloys are ideal for analysis of the EHE: (i) Ni and Pt have a perfect chemical matching. They belong to the same group-10 in the periodic table, have similar electronic [ $(n-1)d^9ns^1$ ], and crystal (fcc) structures and form solid solutions at any concentrations (unlike many binary alloys that are prone to phase segregation [1, 13]). (ii) Pt is characterized by large spin-orbit coupling, needed for the EHE. (iii) Ni has a sharp singularity in the minority d-band near the Fermi surface [14]. Both latter factors amplify the intrinsic EHE in NiPt alloys [4, 5]. (iv) A binary alloy between a magnetic (Ni) and a normal (Pt) metal is the simplest system in which spin-splitting of the electronic system and the ferromagnetic Curie temperature  $T_C$  can be continuously tuned by changing the alloy composition. For  $\text{Ni}_x\text{Pt}_{1-x}$  alloys ferromagnetism appears at the critical Ni concentration  $x_c \simeq 0.4$  [15]. The fact that  $T_C = 0$  at  $x = x_c$  indicates the occurrence of a ferromagnetic quantum phase transition (QPT), driven by quantum rather than thermal fluctuations [16].

Here we study Hall effect in NiPt thin films. It is observed that the OHE remains negative (electron-like) at any composition of the alloy. The EHE is also negative except in the vicinity of the ferromagnetic quantum critical point. Close to the critical point the sign of the extraordinary Hall effect can be changed to positive (hole-like) by tuning either the temperature or the composition of the alloy. We attribute such an “anti-ordinary” Hall effect with opposite signs of the OHE and the EHE to a Berry phase singularity, shifting away from the Fermi energy with increasing ferromagnetic exchange energy. The spectroscopic information contained in the observed anti-ordinary Hall effect indicates its intrinsic (electron-structure related) nature.

NiPt thin films with thicknesses  $\sim 35 - 45$  nm were made by magnetron co-sputtering on oxidized Si wafers at room temperature. The compositions of the films were determined by energy-dispersive X-ray spectroscopy [15]. The films were patterned into Hall bridges using photolithography and ion milling. Resistive measurements were made in a  $^4\text{He}$ -gas flow cryostat with a superconducting solenoid. All Hall measurements were made in field perpendicular to the film. Magnetization measurements were made using a commercial SQUID magnetometer (Quantum Design MPMS 5XL). To avoid complications with the demagnetization factor, the magnetization was measured with the field parallel to the films. More details on sample fabrication, characterization and the experimental setup can be found in Ref. [15].

Figure 1 a-g shows Hall resistivities  $\rho_{xy}(H)$  of NiPt thin films with different concentrations at  $T = 2$  K. The linear-in-field OHE contribution is clearly seen at large fields. It changes only modestly with concentration. Note that for all alloys  $R_0 = d\rho_{xy}/dH$  is negative, which is also the case for pure Ni and Pt [1]. The step-like change of  $\rho_{xy}$  at low fields is due to the EHE and reflects the step-like change of the magnetization  $M(H)$ , shown in Fig. 1h. It is seen that at low Ni concentrations, Fig. 1a,b, the EHE has the same sign as the OHE (at low  $T$  such films are in a frozen cluster-glass state with a perpendicular magnetic anisotropy, leading to a relatively large

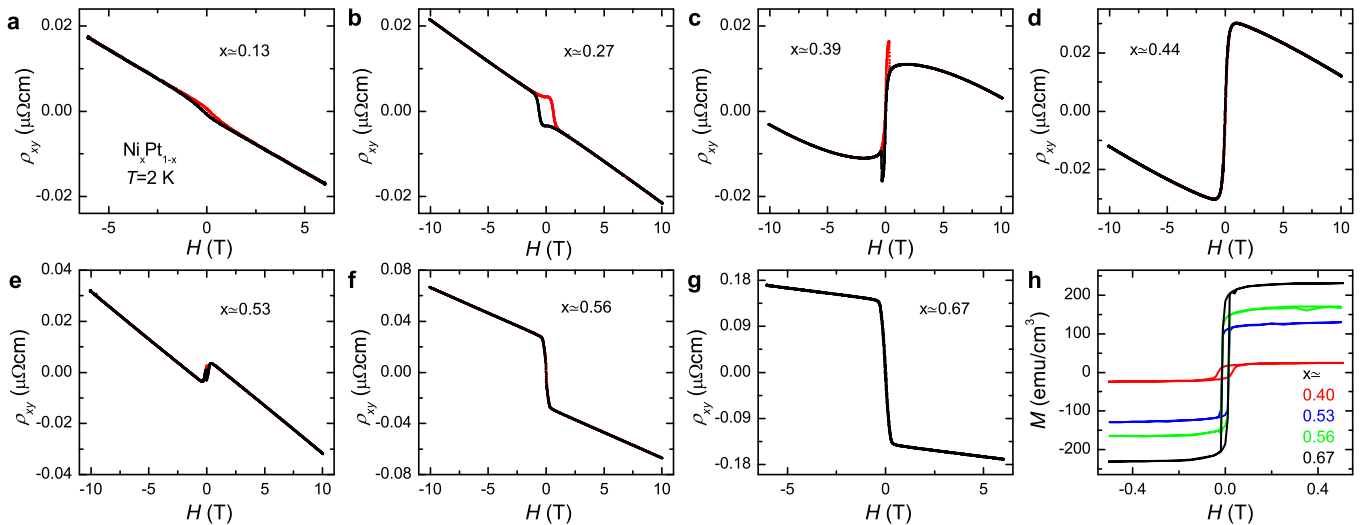


FIG. 1. (Color online). **a-g**, Hall resistivity of  $\text{Ni}_x\text{Pt}_{1-x}$  thin films with different Ni concentrations at  $T = 2$  K for increasing (black) and decreasing (red) fields perpendicular to films. The linear-in-field OHE is clearly seen at large fields. The OHE is electron-like irrespective of concentration. The step-like change of  $\rho_{xy}$  at low fields is due to the EHE. With increasing Ni concentration the EHE changes sign and become hole-like close to the critical ferromagnetic concentration  $x_c \simeq 0.4$ , indicating the occurrence of the anti-ordinary Hall effect. **h**, Magnetization vs. in-plane field  $H$  for films with different Ni concentrations measured at  $T = 2$  K ( $x \simeq 0.40, 0.53$  and  $0.56$ ) and  $10$  K ( $x \simeq 0.67$ ).

hysteresis in  $\rho_{xy}(H)$  [15]). Upon approaching the critical ferromagnetic concentration  $x_c \simeq 0.4$ , Fig. 1c,d, the EHE changes sign and becomes positive, indicating the occurrence of the anti-ordinary Hall effect [5]. With further increase of Ni concentration the positive EHE decreases, almost quenches at  $x \simeq 0.53$  and then again changes sign and becomes negative in Ni-rich alloys, Fig. 1f,g.

Figure 2 shows the  $T$ -variation of the  $\rho_{xy}(H)$  curves for different films. In films with low Ni concentration, Fig. 2a, both the OHE and the EHE are negative at all temperatures. Close to the critical Ni concentration  $x_c \simeq 0.4$  the EHE becomes positive at low  $T = 2$  K, as seen from Fig. 2b, indicating the appearance of the anti-ordinary Hall effect. At a higher Ni concentration  $x \simeq 0.44$ , Fig. 2c, the EHE has a large positive value at low  $T = 2$  K. With increasing  $T$  the positive EHE decreases, acquiring a small negative value before vanishing at high  $T$ . At  $x \simeq 0.53$ , Fig. 2d, the EHE at low  $T = 2$  K is almost quenched, but the large positive EHE is restored at elevated  $T = 100$  K. At higher Ni concentration  $x \simeq 0.56$ , Fig. 2e, the EHE at low  $T$  becomes negative, but the magnitude of the negative EHE decreases with increasing temperature and a small positive EHE reemerges at  $T = 150$  K. Finally at large Ni concentration  $x \simeq 0.67$ , Fig. 2f, the anti-ordinary Hall effect disappears. Here the EHE is again negative at all  $T$  and vanishes upon approaching  $T_C$ .

Figure 3 summarizes composition dependencies of NiPt film characteristics. Figure 3a shows the residual longitudinal resistivity  $\rho_{xx0}$  at  $T = 2$  K and  $H = 0$ . It follows a standard parabolic behavior for binary alloys

(scattering of the data is caused by a varying surface contribution due to different film thicknesses). Figure 3b shows the OHE coefficient at  $T = 2$  K, obtained from the large-field slope of the  $\rho_{xy}(H)$  curves shown in Fig. 1:  $R_0 = d\rho_{xy}/dH_{[H \sim 10 \text{ T}]}$ . It is seen that the OHE remains negative at all concentrations. Figure 3c displays the saturated value of the EHE resistivity at  $T = 2$  K:  $\rho_{\text{EHE}} = \rho_{xy} - (d\rho_{xy}/dH_{[H \sim 10 \text{ T}]})H$ . From Fig. 3c it is clear that the onset of the anti-ordinary Hall effect, indicated by the arrow, appears in the vicinity of the critical Ni concentration  $x_c \simeq 0.4$ .

In Fig. 3d,e, the temperature dependence of the magnetization at  $H = 0.05$  T and the EHE resistivity at  $|H| = 0.16$  T are displayed. The Curie temperature for the films with super-critical Ni concentration is well defined from the onset of magnetization. Figure 3e demonstrates that the EHE also changes sign as a function of temperature at concentrations close to the critical, as seen from Fig. 2b-e.

To understand the origin of the observed sign-reversal of the EHE, we first recollect factors that determine the sign of the Hall effect. The sign of the OHE is determined by the sign on the effective mass of charge carriers, reflecting the curvature of the Fermi surface [1, 2]. From Fig. 3b it is seen that the OHE remains electron-like at all concentrations, indicating that there is no change of the topology for the major part of the Fermi surface. Therefore, the discussed sign change of the EHE in NiPt is qualitatively different from that in binary alloys between metals with hole-like (e.g. Fe or Co) and electron-like (e.g. Cu, Pd, Pt, Au) carriers, in which the sign

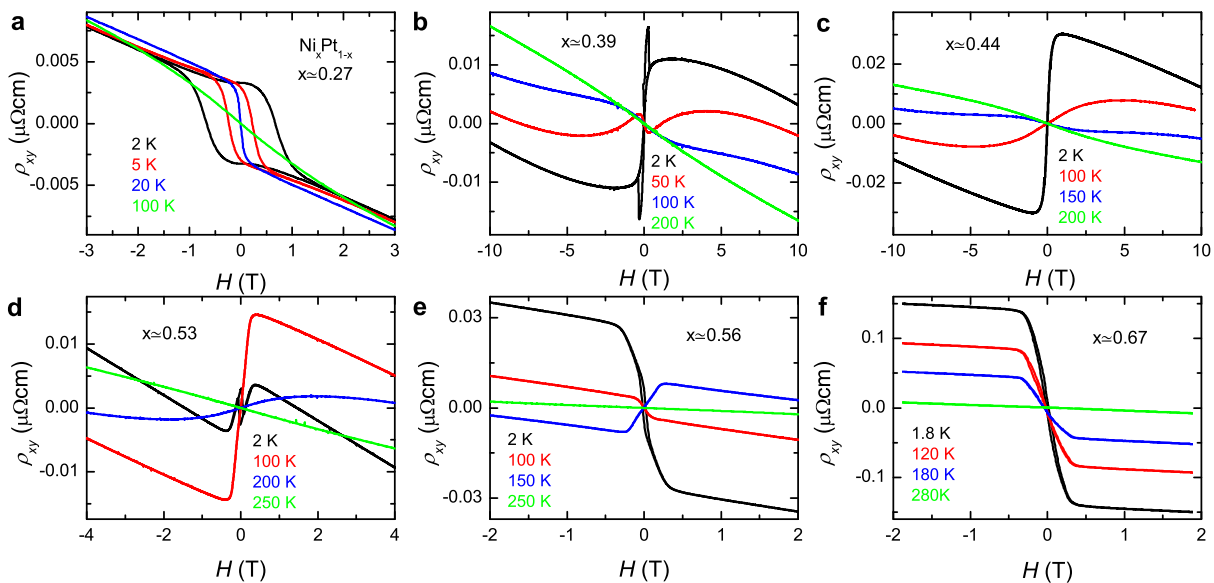


FIG. 2. (Color online). **a-f**,  $T$ -evolution of  $\rho_{xy}$  vs.  $H$  curves for films with Ni concentrations  $x \simeq 0.27$  (**a**),  $0.39$  (**b**),  $0.44$  (**c**),  $0.53$  (**d**),  $0.56$  (**e**) and  $0.67$  (**f**). For films with low (**a**) and high (**f**) Ni concentrations both the OHE and the EHE are electron-like at all temperatures. However, in films with near critical concentration  $x_c \simeq 0.4$  the EHE changes sign to become hole-like at a certain temperature (**b-e**), while the OHE always remains electron-like.

change of both OHE and EHE as a function of composition can be associated with the change of carrier type [1, 4, 5]. In our case we are mixing two electron-like metals from group-10 in the periodic table, with similar crystal and band structures and for which the majority of mobile (s-type) charge carriers remain always electron-like. It is only the EHE that changes sign close to the ferromagnetic quantum critical point  $x = x_c$ ,  $T_C = 0$ .

The sign of the extrinsic skew scattering EHE mechanism [9] may depend on the sign of the interaction with the scatterer (attractive or repulsive). However, the skew scattering can not explain the observed multiple sign reversals of the EHE in our NiPt films as a function of concentration and temperature. For a given set of elements (Ni and Pt) the sign of the interaction should not depend on concentrations or  $T$ . Furthermore, the skew mechanism is significant only in clean materials with low resistivity [3]. Our diluted (both Ni and Pt rich) films, with the lowest resistivities, Fig. 3a, have the same electronic sign of both the OHE and the EHE, Fig. 1a,b,g, i.e., the skew scattering, if present, leads to a negative EHE. Only films with near critical concentrations, that are characterized by fairly large resistivities  $\rho_{xx} \sim 30 - 40 \mu\Omega\text{cm}$ , see Fig. 3a, exhibit the anti-ordinary Hall effect. At those resistivities the intrinsic mechanism is usually dominant [3]. Furthermore, for films with concentrations slightly larger than  $x_c$  the EHE again changes sign to become anti-ordinary with increasing temperature, Fig. 3e, i.e., with increasing scattering rate, clearly indicating that the positive contribution to the EHE is not due to the skew scattering.

Discrimination between the intrinsic [8] and the extrinsic side jump [10] EHE mechanisms is more complicated. Both are scattering-independent and can be connected to the Fermi surface topology, but in a way significantly different from the OHE case. Namely, they are connected to the Berry phase curvature [3–5, 7, 11, 12], rather than the Fermi surface curvature. As a result, the EHE for both mechanisms arises only from singular points occupying small parts of the Fermi surface. However, the two EHE mechanisms may arise from different parts at the Fermi surface and may have different signs [4, 12]. The most important difference for our case is that the amplitude of the extrinsic side-jump EHE is only weakly dependent on parameters of the electronic system and usually maintains the same sign upon varying external parameters [4, 7, 12]. To the contrary, the intrinsic EHE is very sensitive to parameters of the electronic system and may experience significant changes both in the amplitude and even in the sign [4, 17]. Therefore, sign reversal EHE as a function of composition or temperature, observed in a variety of materials [1], is often attributed either to a competition between extrinsic and intrinsic contributions with different signs [7, 18, 19], or solely to the sign change of the intrinsic EHE [3, 5, 17, 20].

As seen from Fig. 3b, the OHE for our NiPt films remains negative at all concentrations, indicating that there is no change of the topology for the major part of the Fermi surface. This brings us to the conclusion that the observed multiple sign changes of the EHE are caused by the intrinsic EHE mechanism, associated with the Berry phase singularity, occupying a relatively small

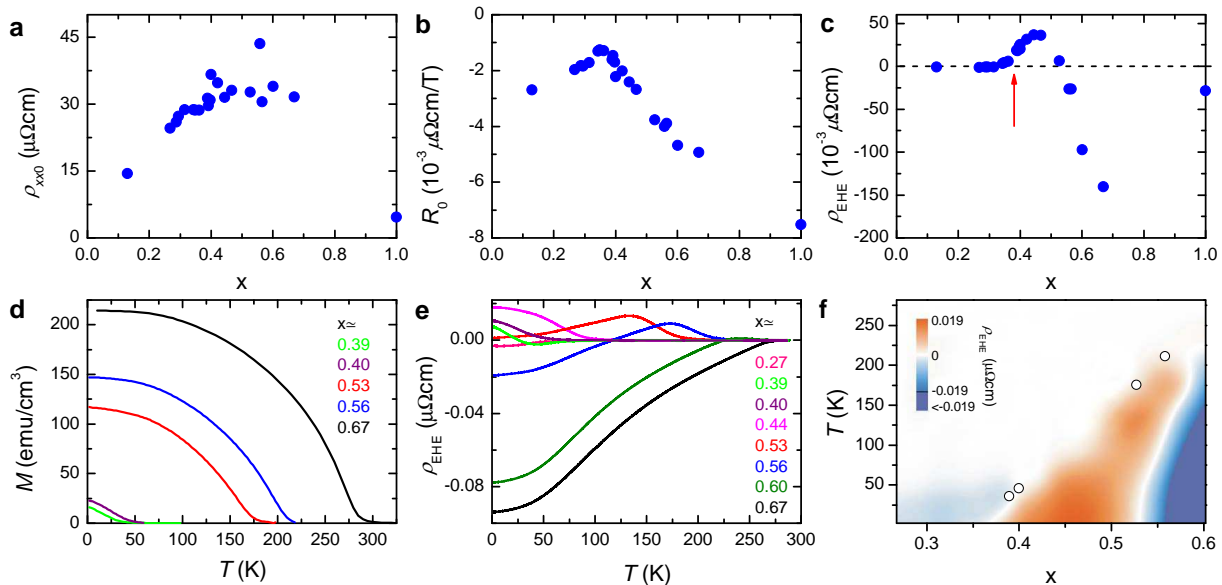


FIG. 3. (Color online). **a-c**, The residual longitudinal resistivity at  $T = 2$  K and  $H = 0$  T (**a**), the OHE coefficient  $R_0$  at  $T = 2$  K (**b**) and the extraordinary Hall resistivity  $\rho_{\text{EHE}}$  measured at  $H = 10$  T and  $T = 2$  K (**c**). Panels **d** and **e** show temperature dependencies of magnetization at  $H = 0.05$  T and the extraordinary Hall resistivity at  $|H| = 0.16$  T for films with different compositions. **f**, The  $T - x$  diagram (color plot) of the extraordinary Hall resistivity obtained from **e**. The anti-ordinary Hall effect appears in the vicinity of the quantum phase transition,  $x_c \simeq 0.4$ ,  $T_C = 0$ . The open circles in **f** indicate  $T_C$  estimated from the onset of  $M(T)$  in **d**.

portion of the Fermi surface. It is qualitatively similar to the explanation of the sign change of the EHE in  $\text{Sr}_{1-x}\text{Ca}_x\text{RuO}_3$  as a function of Ca doping [17]. In that case it was argued that the sign change was simply caused by the increase of the EHE coefficient  $R_1$  with increasing magnetization. However, unlike  $\text{Sr}_{1-x}\text{Ca}_x\text{RuO}_3$ , in NiPt films there is no obvious scaling between  $R_1$  and  $M$  in Eq. (1). This is most clear from the comparison of the  $M(T)$ , Fig. 3d, and  $\rho_{\text{EHE}}(T)$ , Fig. 3e, dependencies; at a similar magnetization the near-critical films have positive EHE, while the rest of the films have negative EHE. Clearly, there is no universal scaling  $R_1(M)$ , but  $R_1$  is varying with Ni concentration.

Figure 3f shows the  $T - x$  diagram of the EHE resistivity for the NiPt films. It is clear that positive EHE emerges at the ferromagnetic QPT,  $x_c \simeq 0.4$ ,  $T_C = 0$ . With increasing Ni concentration  $x > x_c$  the EHE turns negative at low  $T$ , but the positive EHE is restored at an elevated  $T$ . Such a behavior can be understood if the Berry phase singularity, responsible for the sign change of the EHE, crosses the Fermi level at  $x = x_c$  and moves away from the Fermi level at  $x > x_c$ . Since the singularity is lying above the chemical potential at  $x > x_c$ , the anti-ordinary EHE disappears at  $T \rightarrow 0$ . However, it reemerges with increasing temperature, when the singularity is repopulated by thermally excited quasiparticles. In this case the temperature of the maximum anti-ordinary EHE is a measure of the energy shift of the singularity. At all concentrations the maximum occurs

slightly below  $T_C$ , consistent with the assumption that the energy of the singularity is connected with the ferromagnetic exchange energy.

To conclude, we have reported on the unusual “anti-ordinary” Hall effect in NiPt thin films. The phenomenon is attributed to the Berry phase singularity in the spin-polarized d-band part of the Fermi surface. We are able to trace how the singularity moves away from the Fermi level with increasing Ni concentration, in correlation with the increase of the exchange energy. Such spectroscopic information, contained in the anti-ordinary Hall effect clearly indicates that it is of intrinsic, electronic structure-related, nature.

Support from the Swedish Research Council, and the SU-Core facility in Nanotechnology is gratefully acknowledged.

\* Vladimir.Krasnov@fysik.su.se

- [1] C.M. Hurd, *The Hall effect in metals and alloys* (Plenum press, New York-London, 1972).
- [2] D.V. Evtushinsky, *et al. Phys. Rev. Lett.* **100**, 236402 (2008).
- [3] N. Nagaosa, J. Sinova, S. Onoda, A.H. MacDonald, and N.P. Ong, *Rev. Mod. Phys.* **82**, 1539 (2010).
- [4] X. Wang, D. Vanderbilt, J.R. Yates, and I. Souza, *Phys. Rev. B* **76**, 195109 (2007).
- [5] H. Zhang, S. Blügel, and Yu. Mokrousov, *Phys. Rev. B* **84**, 024401 (2011). Note that the term “antiordinary Hall

- effect” in this paper has a somewhat different meaning.
- [6] H. Kontani, T. Tanaka, D.S. Hirashima, K. Yamada, and J. Inoue, *Phys. Rev. Lett.* **102**, 016601 (2009).
  - [7] D. Ködderitzsch, S. Lowitzer, J.B. Staunton, and H. Ebert, *Phys. Stat. Solidi B* **248**, 2248 (2011).
  - [8] R. Karplus, and J.M. Luttinger, *Phys. Rev.* **95**, 1154 (1954).
  - [9] J. Smit, *Physica* **21**, 877 (1955).
  - [10] L. Berger, *Phys. Rev. B* **2**, 4559 (1970).
  - [11] A.A. Kovalev, J. Sinova, and Y. Tserkovnyak, *Phys. Rev. Lett.* **105**, 036601 (2010).
  - [12] J. Weischenberg, F. Freimuth, J. Sinova, S. Blügel, and Yu. Mokrousov, *Phys. Rev. Lett.* **107**, 106601 (2011).
  - [13] Note that surface segregation in ordered NiPt alloy is possible, see L.V. Pourovskii, A.V. Ruban, B. Johansson, and I.A. Abrikosov, *Phys. Rev. Lett.* **90**, 026105 (2003).
  - [14] A.I. Lichtenstein, M.I. Katsnelson and G. Kotliar, *Phys. Rev. Lett.* **87**, 067205 (2001).
  - [15] T. Golod, A. Rydh, and V. M. Krasnov, *J. Appl. Phys.* **110**, 033909 (2011).
  - [16] H. v. Löhneysen, A. Rosch, M. Vojta, and P. Wölfle, *Rev. Mod. Phys.* **79**, 1015 (2007).
  - [17] R. Mathieu, *et al. Phys. Rev. Lett.* **93**, 016602 (2004).
  - [18] S.A. Baily, and M.B. Salamon, *Phys. Rev. B* **71**, 104407 (2005).
  - [19] J.G. Checkelsky, M. Lee, E. Morosan, R.J. Cava, and N.P. Ong, *Phys. Rev. B* **77**, 014433 (2008).
  - [20] J. Ye, *et al. Phys. Rev. Lett.* **83**, 3737 (1999).